

Error sources in single-clinopyroxene thermobarometry and a mantle geotherm for the Novinka kimberlite, Yakutia

Luca Ziberna^{a,b,*}, Paolo Nimis^b, Dmitry Kuzmin^{c,d}, Vladimir G. Malkovets^{c,d}

^a School of Earth Sciences, University of Bristol, Wills Memorial Building, Queen's Road, Bristol BS8 1RJ, United Kingdom

^b Dipartimento di Geoscienze, Università di Padova, Via G. Gradenigo 6, 35131 Padova, Italy

^c V. S. Sobolev Institute of Geology and Mineralogy, Siberian Branch of Russian Academy of Sciences, 3 Koptuyga prospect, Novosibirsk 630090, Russia

^d Novosibirsk State University, 2 Pirogova Str., Novosibirsk 630090, Russia

ABSTRACT

A new suite of 173 clinopyroxene grains from heavy-mineral concentrates of the diamondiferous Novinka kimberlite (Upper Muna field, Yakutia) has been analyzed for major and minor elements with an electron microprobe to perform a thermobarometric study and model the thermal structure of the Proterozoic Upper Muna lithospheric mantle. Scrupulous evaluation of propagation of analytical uncertainties on pressure estimates revealed that (i) the single-clinopyroxene geobarometer can be very sensitive to analytical uncertainties for particular clinopyroxene compositions, and that (ii) most clinopyroxenes from Novinka have compositions that are sensitive to analytical uncertainties, notwithstanding their apparent compositional suitability for single-clinopyroxene thermobarometry based on previously proposed application limits. A test on a variety of mantle clinopyroxenes containing different proportions of the sensitive elements Cr, Na and Al allowed us to identify clinopyroxene compositions that produce unacceptably high propagated errors and to define appropriate analytical conditions (i.e., higher beam currents and longer counting times for specific elements) that allow precise P – T estimates to be obtained for sensitive compositions. Based on the results of our analytical test, and taking into account the intrinsic limitations of the single-

clinopyroxene thermobarometer, we have designed a new protocol for optimum thermobarometry, which uses partly revised compositional filters. The new protocol permits precise computation of the conductive paleogeotherm at Novinka with the single-clinopyroxene thermobarometer of Nimis and Taylor (2000). Thermal modeling of the resulting P – T estimates indicates a ~ 34 -mW/m² surface heat flow, a thermal lithosphere thickness of ~ 225 km, and an over 100 km-thick ‘diamond window’ beneath Novinka in the middle Paleozoic (344–361 Ma). We estimate that appropriate analytical conditions may extend the applicability of single-clinopyroxene thermobarometry to over 90% of clinopyroxene-bearing garnet peridotites and pyroxenites and to $\sim 70\%$ of chromian-diopside inclusions in diamonds. In all cases, application to clinopyroxenes with $\text{Cr}/(\text{Cr} + \text{Al})_{\text{mol}} < 0.1$ is not recommended. We confirm the tendency of the single-clinopyroxene barometer to progressively underestimate pressure at $P > 4.5$ GPa.

Keywords: Geobarometry, Chromian diopside, Lithospheric mantle, Palaeogeotherms

INTRODUCTION

Over the last few decades, thermobarometry of rocks and minerals derived from Earth’s mantle has represented a fundamental tool for the evaluation of the thermal state and structure of sub-craton and off-craton lithospheric sections (e.g., Boyd 1973, 1984; O’Reilly and Griffin 1985; Boyd et al. 1997; Kopylova et al. 1998; Griffin et al. 1999, 2002, 2004; Lazarov et al. 2009; Janney et al. 2010), as well as for the assessment of their diamond potential (e.g., Read et al. 2004; Read and Janse 2009; Cookenboo and Grütter 2010). Deep-seated mantle samples mostly occur as discrete xenoliths or xenocrysts in alkaline magmatic rocks, as isolated grains in sediments derived from their weathering and disruption, and as monomineralic or polymineralic inclusions in kimberlite- and lamproite-borne diamonds. Only the relatively rare discrete xenoliths and polymineralic inclusions in diamonds may be suitable for conventional, two-phase thermobarometry. Single-mineral thermometer–barometer pairs, such as those available for peridotitic garnet and clinopyroxene (Ryan et al. 1996; Nimis and Taylor

2000; Grütter et al. 2006), permit thermobarometric surveys to extend across copious data for mantle-derived xenocrysts. Although with some limitations concerning their reliability and applicability (e.g., Cookenboo and Grütter 2010), the single-mineral methods have enabled the vertical and horizontal mapping of the lithospheric mantle to an extent far beyond that achievable with xenoliths alone (e.g., Griffin et al. 1999, 2002, 2004; Malkovets et al. 2007; Ashchepkov et al. 2008; Grütter and Tuer 2009; Lehtonen et al. 2009; Nimis et al. 2009; Zozulya et al. 2009).

The single-clinopyroxene thermobarometer of Nimis and Taylor (2000) is one of the most used and most reliable single-mineral methods for thermobarometry of disaggregated mantle xenoliths (Nimis 2002; Putirka 2008; Grütter 2009; Nimis and Grütter 2010), though its application requires judicious filtering of appropriate clinopyroxene compositions, as well as careful evaluation of the errors associated with calculated temperatures and pressures. Empirically determined compositional filters for single-clinopyroxene thermobarometry were proposed by Nimis and Taylor (2000) and endorsed by Grütter (2009), and low-quality microprobe data were highlighted as responsible for unreliable clinopyroxene thermobarometry outcomes (Grütter 2009; Mather et al. 2011). However, the source of the decreased reliability of single-clinopyroxene thermobarometry for particular compositions has never been investigated in detail. In this contribution, we assess the various sources of error that may affect single-clinopyroxene barometry and propose a new protocol for optimal single-clinopyroxene thermobarometry which specifically considers analytical errors and uses partly revised compositional filters. We then use our results to define a precise conductive geotherm for the diamondiferous Novinka kimberlite, Yakutia, based on high-quality electron microprobe analyses of 97 chromian diopside xenocrysts, selected out of an initial suite of 173 chromian diopside grains. We show that previously proposed compositional filters are sufficient for routine evaluation of mantle geotherms using data for large populations of mantle-derived clinopyroxenes, but that high-quality chemical analyses significantly improve the precision of the individual P - T estimates for fairly common chromian diopside compositions.

GEOLOGICAL OUTLINE AND PRELIMINARY SAMPLE SELECTION

The Upper Muna kimberlite field is located at the northern limb of the Markha Terrane, in the central part of the Siberian Craton, and is one of the thirteen fields that form the SW–NE Daldyn–Olenek kimberlite corridor (Fig. 1). This kimberlite field is composed of twenty kimberlite bodies intruded in the Upper Cambrian limestones of the sedimentary cover of the Siberian Platform and is related to the Late Devonian–Early Carboniferous episode of kimberlite magmatism on the Siberian platform (Davis et al. 1980; Agashev et al. 2004; Sun et al. 2014). Recent age determinations gave a narrow interval of kimberlite formation from 361 to 344 Ma (Griffin et al. 1999; Levchenkov et al. 2005; Lepekhina et al. 2008a,b; Malkovets VG, unpublished data). For the Novinka kimberlite, SHRIMP analyses of groundmass perovskites gave a U–Pb age of 355 ± 11 Ma (Lepekhina et al. 2008b). One of the striking features of the Upper Muna kimberlite field is that most of the bodies are diamondiferous. All the kimberlite bodies are characterized by abundant fresh deep-seated xenocrysts and xenoliths, but eclogite and crustal xenoliths are very rare.

The samples for this study were collected from five sites in the quarry left after bulk sampling inside the contour of the pipe at the present surface and are believed to be a representative mixture of all exposed kimberlite types presently recognized at Novinka. A total of 173 fresh green clinopyroxene grains were picked from the 0.3 to 1.5-mm fraction of heavy-mineral concentrates separated using bromoform at the VS Sobolev Institute of Geology and Mineralogy, Siberian Branch Russian Academy of Sciences, Novosibirsk, Russia. Preliminary major element analyses were performed on these grains using a JEOL Superprobe JXA-8200 electron microprobe (hereafter, EMP) housed at the Max Planck Institute for Chemistry, Mainz, Germany. Operating conditions and compositions for all 173 grains are reported in the Supplementary Table S1.

OPTIMIZED PROTOCOL FOR PRECISE SINGLE-CLINOPYROXENE THERMOBAROMETRY

Source of errors and compositional filters

The single-clinopyroxene thermobarometer uses a combination of the enstatite-in-Cpx thermometer and Cr-in-Cpx barometer (Nimis and Taylor 2000). The enstatite-in-Cpx thermometer has proved a top-quality method when compared to other mantle geothermometers (Nimis and Grütter 2010) and has limited sensitivity to analytical uncertainties (Nimis 2002). The Cr-in-Cpx barometer suffers from two major drawbacks: i) evaluations against experiments have shown progressive underestimation of the equilibrium pressures above ca. 4.5 GPa (up to 0.6–1.0 GPa at 7.0 GPa; Nimis 2002); ii) deviations from results of orthopyroxene–garnet barometry on the same xenolith samples can be very large for clinopyroxenes characterized by low values of $a_{\text{Cr}} = \text{Cr} - 0.81 \cdot (\text{Na} + \text{K}) \cdot \text{Cr} / (\text{Cr} + \text{Al})$ atoms per 6-oxygen formula unit (hereafter apfu), which is the main building block in the barometer formulation (Fig. 2). Low a_{Cr} values at high P/T ratios in the calibration database, a molar volume change for the reaction involving garnet and clinopyroxene (cf. equation 1 in Nimis and Taylor 2000) less than one-half that of common orthopyroxene-based barometers (cf. Brey et al. 1990), and the intrinsic limitations of being an empirical single-mineral method account for the lower precision of the Cr-in-Cpx barometer (cf. Figs. 1c,d in Grütter 2009). More generally, these drawbacks may explain why P – T estimates using the single-clinopyroxene methods are often more scattered compared to those using conventional thermobarometers (cf. Stachel and Harris 2008; Eaton et al. 2009; Shirey et al. 2013).

Apart from the above issues, safe application of the single-clinopyroxene method requires a careful selection of the samples, in order to exclude compositions outside the range used for the calibration or too sensitive to analytical uncertainties. Grütter (2009) compiled and partly modified compositional and related filters designed by various authors that serve as a useful ‘cookbook’ to eliminate unwarranted data from consideration for P – T calculations. The filters include: (i) total cations per 6 oxygens in the range 3.96–4.04, slightly more permissive than the 3.98–4.02 range advised by Nimis and Taylor (2000); (ii) Cr_2O_3 vs Al_2O_3 relationships within the garnet-peridotite field of Ramsay and

Tompkins (1994); (iii) Al_2O_3 vs MgO relationships within the high-Al field of Nimis (1998); (iv) $Cr\#$ in the range 0.06–0.50; (v) $a_{Cr} \geq 0.003$ apfu. Filter (i) serves to exclude obviously poor-quality analyses, which may result from poor EMP standardization, bad sample preparation, contamination from inclusions, etc. In this work we revert to the more restrictive 3.98–4.02 cation range to promote high-quality P – T estimates for individual clinopyroxene grains. Filters (ii) and (iii) serve to exclude clinopyroxenes that may not have been in equilibrium with garnet. Filters (iv) and (v) exclude compositions falling well outside the range of the experiments used for the calibration of the Cr-in-Cpx barometer, which included clinopyroxenes with $Cr\# = 0.09$ – 0.44 , and $a_{Cr} = 0.003$ – 0.087 apfu (Nimis and Taylor 2000). As originally suggested by Nimis and Taylor (2000), the removal of clinopyroxenes with $a_{Cr} < 0.003$ apfu should also help to exclude compositions that are too sensitive to propagation of analytical errors. We will show that filters (iv) and (v) require revision.

Figure 2 shows that the threshold $a_{Cr} \geq 0.003$ apfu suggested by Nimis and Taylor (2000) and adopted by Grütter (2009) may be too optimistic: at $a_{Cr} = 0.010$ apfu, deviations from the orthopyroxene–garnet pressures calculated for the same well-equilibrated mantle xenoliths may be as high as ± 1.0 GPa, reaching ± 3.0 GPa for $a_{Cr} < 0.003$ apfu. This shortcoming is particularly relevant for the study of Novinka chromian diopsides. Based on preliminary microprobe analyses of 173 grains (Supplementary Table S1), 118 grains satisfy the compositional criteria for derivation from garnet peridotite [i.e., filters (ii) and (iii)], with 39 of 118 (33%) having $a_{Cr} \leq 0.003$ apfu, and 107 of 118 (91%) having $a_{Cr} \leq 0.010$ apfu. Observing the latter threshold would therefore render most of our Novinka samples unsafe for thermobarometry. In principle, the decreased precision of the Cr-in-Cpx barometer at low a_{Cr} may be due to an oversimplified treatment of Cr equilibria between clinopyroxene and garnet or it may reflect an excessive sensitivity of the method to analytical errors or to departures from chemical equilibrium. Mather et al. (2011) made a semi-quantitative evaluation of the influence of analytical errors, but they did not account for their dependence on absolute element concentrations and

analytical conditions (cf. Potts 1983 and Appendix of this work). In the present work, we have made an analytical test to quantitatively assess the propagation of analytical errors on pressure estimates (see Appendix for details): multiple EMP analyses on compositionally diverse clinopyroxenes using different analytical conditions demonstrated that (i) the decreased precision of the Cr-in-Cpx barometer for clinopyroxenes with low a_{Cr} values is largely related to propagation of analytical errors, (ii) the analytical errors, as expected, increase smoothly with decreasing beam current and counting times, and (iii) the propagated P uncertainties are negatively correlated with the clinopyroxene a_{Cr} parameter and positively correlated with the clinopyroxene $\text{Cr}/(\text{Cr} + \text{Al})$ molar ratio ($\text{Cr}\#$) (Fig. 3). Therefore, the $a_{\text{Cr}}/\text{Cr}\#$ parameter, rather than the previously used a_{Cr} parameter, is a more reliable indicator of the sensitivity of single-clinopyroxene barometry to analytical uncertainties. Minimum conditions for electron microprobe analysis were thus defined for different values of the $a_{\text{Cr}}/\text{Cr}\#$ parameter (Table A2), which maintain propagation of analytical uncertainties within acceptable limits (defined here as ± 0.25 GPa).

A further assessment of the importance of analytical errors on Cr-in-Cpx P estimates can be made using mantle xenoliths as test cases. Based on the results of our analytical tests (see Appendix), we have refined the database of well-equilibrated xenoliths of Nimis and Grütter (2010) by excluding those clinopyroxene analyses for which the estimated P uncertainties were unsatisfactorily high. For each record, the analytical errors on Al, Cr, and Na concentrations in the clinopyroxene were calculated taking into account the analytical conditions used for the analysis as reported in the source papers, and the corresponding P uncertainties were calculated through error propagation. If the reported analytical conditions did not match exactly any of those utilized here, the errors were estimated by interpolation of values obtained by assuming lower and higher beam currents or counting times. For records for which analytical details had not been reported, we cautiously assumed the beam current and counting times to be the lowest (i.e., 15 nA, 10 s peak, 10 s background). The records for which the model P uncertainties were greater than ± 0.25 GPa were discarded. Clearly, the model P uncertainties may not

be strictly accurate, since different analytical equipments were used for the analyses. However, the above screening certainly excluded most of the records for which single-clinopyroxene P – T estimates are probably unreliable. Figure 4 shows that the discrepancies between Cr-in-Cpx and orthopyroxene–garnet pressures are greatly reduced for the refined database, especially at pressures above 3 GPa, thus supporting the major role of propagation of analytical errors on P uncertainties. At lower pressures, significant deviations are still observed only for a few samples with $Cr\# < 0.1$ (Fig. 4b), which suggests poor reliability of the Cr-in-Cpx barometer for these low- $Cr\#$ compositions. This may be related to the fact that the Cr-in-Cpx barometer was calibrated on 120 experimental clinopyroxenes with $Cr\#$ in the range 0.09–0.44, with only 6 of them having $Cr\# < 0.1$ (Nimis and Taylor 2000). The original minimum threshold of 0.06 for $Cr\#$ suggested by Grütter (2009) thus appears to be too permissive. Examination of Figure 4b also reveals that clinopyroxenes with $Cr\#$ as high as 0.65 do not show any systematic deviation from orthopyroxene–garnet P . This suggests that the upper limit for $Cr\#$ of 0.50 proposed by Grütter (2009) is excessively restrictive, despite the fact that the Cr-in-Cpx barometer was calibrated on clinopyroxenes with $Cr\# \leq 0.44$.

An additional problem when investigating loose mineral grains is to assess whether the clinopyroxene was in equilibrium with orthopyroxene, a condition necessary for single-clinopyroxene thermometry. Recognition of orthopyroxene-saturated samples is not straightforward and was not explicitly addressed by Grütter (2009). Based on the above considerations, we propose a partly revised protocol for sample selection, which takes into account both the intrinsic limitations of the single-clinopyroxene thermobarometers and the uncertainties related to propagation of analytical errors.

(1) *General quality test of EMP analysis*: total cations per 6 oxygens in the range 3.98–4.02. Less restrictive limits, such as those suggested by Grütter (2009), might be adopted in some cases, but a possible increase of scatter around geotherms should be considered.

(2) *General equilibrium test*: grains exhibiting significant zoning, suggesting disequilibrium, should generally be discarded.

(3) *Verification of equilibrium with garnet*: Cr_2O_3 vs Al_2O_3 relationships within the garnet-peridotite field of Ramsay and Tompkins (1994), i.e., $\text{Cr}_2\text{O}_3 > 0.5 \text{ wt\%}$ and $\text{Al}_2\text{O}_3 \leq 4.0 \text{ wt\%}$ (if $\text{Cr}_2\text{O}_3 < 2.25 \text{ wt\%}$) or $\leq 5.0 \text{ wt\%}$ (if $\text{Cr}_2\text{O}_3 > 2.25 \text{ wt\%}$). This restriction may produce false negatives. The reliability of single-clinopyroxene methods for anomalously Cr_2O_3 -rich compositions ($\text{Cr}_2\text{O}_3 > 5.0 \text{ wt\%}$) is unknown and therefore these compositions should be used with caution.

(4) *Further refinement of (3)*: Al_2O_3 vs MgO relationships within the high-Al field of Nimis (1998), i.e., $\text{Al}_2\text{O}_3 \geq 0.7 \text{ wt\%}$ and $\text{Al}_2\text{O}_3 \geq 12.175 - 0.6375 \cdot \text{MgO wt\%}$ (this parametrization is taken directly from Fig. 3 in Nimis 1998; the slightly different formula suggested by Grütter 2009 provides almost identical results). False negatives may be produced also in this case, especially among diamond-facies samples (cf. Fig. 3 in Nimis 1998).

(5) *Rejection of compositions with ‘unsafe’ Cr# values*: Cr# in the range 0.10–0.65 (replacing the range 0.06–0.50 of Grütter 2009); Cr# values in the range 0.50–0.65 should still be used with caution because of limited testing in this compositional range.

(6) *Recognition of compositions sensitive to analytical uncertainties*: $a_{\text{Cr}}/\text{Cr\#} > x$, where x is a function of EMP analytical conditions. Table A2 provides a general guideline for determining x , although its value may be varied for different analytical equipments based on personal experience. This filter replaces the filter $a_{\text{Cr}} \geq 0.003 \text{ apfu}$ of Nimis and Taylor (2000) and Grütter (2009). If $a_{\text{Cr}}/\text{Cr\#} \leq 0.011 \text{ apfu}$, the clinopyroxenes should generally be discarded; if $0.011 < a_{\text{Cr}}/\text{Cr\#} \leq 0.024 \text{ apfu}$, high-quality analyses are recommended; if $a_{\text{Cr}}/\text{Cr\#} > 0.024$, propagation of analytical errors is predictably small and therefore routine analyses can safely be used. The range for $a_{\text{Cr}}/\text{Cr\#}$ in the experiments used to calibrate the Cr-in-Cpx barometer of Nimis and Taylor (2000) was 0.016–0.393, therefore excluding compositions with $a_{\text{Cr}}/\text{Cr\#} \leq 0.011 \text{ apfu}$ will also avoid large extrapolations outside the calibration range.

(7) *Verification of equilibrium with orthopyroxene.* This cannot be obtained through simple compositional filters. In general, $\text{Ca}/(\text{Ca} + \text{Mg})_{\text{mol}}$ ratios > 0.5 should be considered as suspicious, as a very small proportion of orthopyroxene-saturated chromian diopsides (ca. 1%) lie above this value. A very low estimated T (e.g., $< 600^\circ\text{C}$) would also be a strong indication that the diopside was not in equilibrium with orthopyroxene, which implies underestimation of T using the enstatite-in-Cpx thermometer and, consequently, underestimation of the Cr-in-Cpx P . Following Nimis and Grütter (2010), a cut-off at $T > 700^\circ\text{C}$ provides a safer selection of clinopyroxenes for which enstatite-in-Cpx temperatures should be sufficiently reliable.

(8) *Identification of potential outliers.* As recommended by Grütter (2009), final examination of P – T plots for a given locality may help to distinguish outliers departing off the general trend, which may conveniently be excluded for the determination of mantle geotherms.

Application to Novinka clinopyroxenes

For the purposes of this study, we used the preliminary analyses of Novinka clinopyroxenes (Jeol Superprobe, Mainz; Supplementary Table S1) only for a first compositional screening aimed to eliminate obviously unsuitable analyses. We excluded 55 clinopyroxenes plotting outside the ‘garnet peridotite’ field of Ramsay and Tompkins (1994), which may not be equilibrated with garnet, and 5 clinopyroxenes showing very low enstatite contents [$\text{Ca}/(\text{Ca} + \text{Mg})_{\text{mol}} > 0.5$], which are unlikely to be equilibrated with orthopyroxene. In addition, 16 grains that contained abundant melt inclusions, which likely indicate severe interaction with the host kimberlite magma, were also discarded.

The remaining 97 grains were re-analysed using a CAMECA SX-50 electron microprobe (EMP; IGG–CNR, Padua, Italy) (see Appendix for details). Compositional data were first collected using a *routine* analytical procedure, which employed an accelerating voltage of 20 kV, a beam current of 15 nA, and counting times of 10 s for peak and 10 s for background (i.e., 5 s on each side of the peak), for all elements. Further filtering based on the newly revised protocol was then applied to the results of the

routine analyses. We discarded 5 grains showing significant zoning, 9 grains plotting outside the high-Al field of Nimis (1998) and 9 grains showing $a_{Cr}/Cr\# < 0.011$. We then re-analyzed 56 clinopyroxenes with $0.011 < a_{Cr}/Cr\# \leq 0.024$ using higher beam current (40 nA) and counting times (40 sec for both peak and background) for Al, Cr and Na, and routine EMP conditions for the other elements. Pressures and temperatures were calculated with the thermobarometers of Nimis and Taylor (2000) using the averages of five point analyses. The major element compositions of the peridotitic clinopyroxenes determined using both the routine and the optimized analytical conditions and the relative P – T estimates are reported in the Supplementary Table S2.

RESULTS

Based on the preliminary analyses of the 173 clinopyroxenes (Supplementary Table S1), the majority of the grains (68%) fall into the low-Al, ‘garnet peridotite’ field of Ramsay and Tompkins (1994). About one fourth of these, however, show relationships between Al_2O_3 and MgO contents that are compatible also with an origin from garnet-free, metasomatised lherzolites (cf. Nimis 1998). Another 4% fraction of the ‘garnet peridotite’ grains shows high CaO contents (>22 wt.%), high $Ca/(Ca + Mg)_{mol}$ ratios (>0.5) and excessively low estimated T (<500 °C) and can be classified as ‘wehrlitic’. A relatively large number of the studied grains (29%) have Cr_2O_3 contents lower than 0.5 wt.%, which would classify them as either ‘eclogitic’ or ‘megacrystic’ (Ramsay and Tompkins 1994). The Na_2O content in these low-Cr grains is generally low to very low (mostly <2.5 wt.%), which is more consistent with a megacrystic/pyroxenitic origin. A very small number of grains (2%) have relatively high Al_2O_3 contents (4.6–5.4 wt.%) and fall in the spinel peridotite field of Ramsay and Tompkins (1994).

Grey symbols in Figure 5a show the results of the thermobarometric study of the 97 selected clinopyroxenes using the routine analyses obtained with the CAMECA SX50 (Padua). As expected from the low a_{Cr} values of most clinopyroxenes, the P – T estimates obtained using routine analyses

show considerable scatter, especially at $P > 5.0$ GPa (Fig. 5a). Depending on the preferred model geotherm shape, minor to very large thermal perturbations (up to several hundred degrees) may be inferred near the base of the lithosphere. Adopting the revised filtering protocol proposed in this work and using 56 high-quality analyses for clinopyroxenes with $0.011 < a_{Cr}/Cr\# \leq 0.024$, the P - T scatter is considerably reduced (black symbols in Fig. 5a). Ten samples with $Cr\# > 0.50$ and as high as 0.63 do not show any deviation from the overall trend, which supports the reliability of single clinopyroxene thermobarometry for these compositions (cf. also Fig. 4). The refined thermobarometric estimates ($N = 74$) span the P - T range 2.3–6.5 GPa and 660–1390 °C, with the majority of the clinopyroxenes falling in the diamond stability field (Fig. 5a). Trimming the data at $T > 700$ °C does not produce any reduction in the overall scatter. A gap is observed in the pressure range 3.3–3.9 GPa, which could be related to a sampling bias of the kimberlite or to absence of clinopyroxene-saturated assemblages in the mantle in this pressure interval.

For the sake of comparison, Figure 5b shows the results of the thermobarometric study of the same 97 clinopyroxenes, but adopting Grütter's (2009) original filters for $Cr\#$ ($0.06 < Cr\# < 0.5$) and a_{Cr} (≥ 0.003 apfu) and using routine analyses for all samples. The results show a marginal increase of scatter and an overall shift of the high- P samples (> 4.0 GPa) to slightly higher P , the average difference being ca. 0.2 GPa. However, differences in P - T estimates for individual grains (routine vs. high-quality analyses) are as high as +0.5 GPa and +50 °C and the total number of 'accepted' clinopyroxenes is reduced to 67.

THERMAL STATE AND THICKNESS OF THE UPPER MUNA LITHOSPHERIC MANTLE

Much of what is known about the thermal state of the mantle beneath the Siberian craton comes from studies of xenoliths from the Daldyn field (Fig. 1), and in particular from the Udachnaya kimberlite. Conventional thermobarometry of mantle xenoliths from this kimberlite indicates low geothermal gradients, corresponding to a surface heat flow of 35–40 mW/m² based on the conductive model of

Pollack and Chapman (1977) (hereafter PC77), and deep lithospheric mantle roots (~ 220 km) (Griffin et al. 1996; Boyd et al. 1997; Pokhilenko et al. 1999; Ionov et al. 2010; Goncharov et al. 2012; Agashev et al. 2013; Doucet et al. 2013). Variations in available estimates of the (conductive) mantle geotherm depend in part on the different combinations of thermobarometers used by the different authors and in part on a significant scatter in the reported P – T estimates.

Additional slices of information on the Daldyn field and on the nearby Alakit and Upper Muna fields (Fig. 1) were provided by Griffin et al. (1999), who applied the Ni-in-garnet thermometer and Cr-in-garnet barometer (Ryan et al. 1996) to large suites of garnet xenocrysts. Their results suggest a cool geotherm (35 mW/m^2) and a chemical lithosphere thickness of ~ 240 km for the Alakit mantle section, similar to that in the Daldyn mantle section, but a slightly higher geotherm (38 mW/m^2) and a thinner lithosphere (~ 210 km) for the more northeasterly Upper Muna mantle section. The main limitation of the garnet-based method is that reliable pressure estimates can only be retrieved for Cr-saturated garnets (i.e., garnets in equilibrium with chromite). If this condition is not satisfied, only minimum pressures can be estimated. Therefore, a geotherm is typically obtained by interpolating maximum P estimates determined for each T recorded by a large number of grains. Scatter of individual P – T points and intrinsic uncertainties in the empirical thermobarometer calibrations (Ryan et al. 1996; Canil 1999), however, may limit the accuracy of the interpolation. Moreover, since Cr-saturated garnets are relatively rare in kimberlites and their vertical distribution is not uniform (Griffin et al. 2002; Malkovets et al. 2007), localized thermal perturbations are not easily recognized. More recent P – T estimates for the Upper Muna field were provided by Ashchepkov et al. (2010), using combinations of different thermobarometers. The results were ambiguous, because of the very large scatter of P – T estimates and evident inconsistencies among the different thermobarometers used (see Figs. 18 to 20 in Ashchepkov et al. 2010).

Our P – T data for clinopyroxenes provide independent constraints on the thermal state of the Upper Muna lithospheric mantle at the time of eruption of the Novinka kimberlite. Figure 5 shows that the

low- T (< 1100 °C) clinopyroxenes align along the 40-mW/m² model conductive geotherm of PC77, which is slightly warmer than the ‘garnet geotherm’ defined by Griffin et al. (1999) for the Upper Muna field (38 mW/m²). This is consistent with the observations of Grütter et al. (2006), who demonstrated that the Ni-in-garnet method of Ryan et al. (1996) adopted by Griffin et al. (1999) tends to underestimate mantle geotherms by ~ 2 mW/m². An apparent inflection of the geotherm is observed at $T > 1100$ °C and $P > 5.5$ GPa, with P – T data plotting on or slightly above the 44-mW/m² model conductive geotherm (Fig. 5a). This apparent inflection may partly be an artifact caused by the known P underestimation at high pressures of the Cr-in-Cpx geobarometer (cf. Nimis 2002; see also next Section). More importantly, the still widely used PC77 reference model predicts a stronger curvature of geotherms compared with recent thermal models (cf. Hasterok and Chapman 2011; Mather et al. 2011), and could suggest deviation from a conductive thermal gradient even in unperturbed mantle sections.

To derive a robust geotherm for the Upper Muna field, we have fitted the clinopyroxene P – T data using the FITPLOT program (McKenzie and Bickle 1988; McKenzie et al. 2005), as upgraded by and described in Mather et al. (2011). Different from the PC77 reference geotherms, this program allows computing the change in temperature with depth within the thermal boundary layer, allows varying the crustal thickness and heat production in the crust and mantle, and includes updated models for the temperature dependence of thermal conductivity. Moreover, the surface heat flow is an output of the fitting procedure and not a fixed input value that is used to generate a geotherm. We assumed a crustal thickness of 56 km based on Manakov’s (2002) seismic model for the Siberian craton. The mean heat production in the crust was assumed to be $0.36 \mu\text{W}/\text{m}^3$, in agreement with data reported in Rosen et al. (2009) for the Anabar shield. The heat production rate in the upper mantle was imposed at $0.0 \mu\text{W}/\text{m}^3$ and the potential T for the asthenospheric isentrope was set at 1315 °C, following Mather et al. (2011). The thermal conductivity was assumed to be $2.5 \text{ W}/\text{m}\cdot\text{K}$ throughout the crust. In the mantle, we used the thermal conductivity for olivine at (P , T) of Osako et al. (2004).

Comparison of the clinopyroxene P – T data with the calculated geotherm (Fig. 6a) shows an excellent agreement in the intermediate P – T region, with a residual ‘inflection’ at high P – T . The magnitude of this inflection is compatible with the above-mentioned underestimation of the Cr-in-Cpx barometer at high P (Nimis 2002; see also next Section). Therefore, we interpret the smooth high- P – T inflection as an artifact. To minimize the potential bias due to P underestimation at high P and derive a more refined geotherm, we have re-fitted the P – T data by excluding data plotting above 5.5 GPa. Trimming the data did not produce significant changes in the model geotherm, excepting for an obvious significant reduction of the xenolith misfit and a very slight increase in the calculated lithospheric thickness, as defined by the intersection of the conductive geotherm with the mantle isentrope (Fig. 6b). The agreement between the trimmed P – T data and the model is excellent. The resulting surface heat flow is 34 mW/m² and the base of the thermal lithosphere is at 225 km, corresponding to a T of 1436 °C. The base of the Mechanical Boundary Layer (McKenzie and Bickle 1988) is at 204 km depth, corresponding to a T of 1355 °C. Hasterok and Chapman’s (2011) geotherm model, which uses a more generalized heat production model for the continental lithosphere, would also provide a good fit to the P – T data and would only suggest a slightly higher surface heat flux of 37 mW/m². The computed heat flow is slightly lower than that estimated by simple visual comparison with the PC77 model geotherms (Fig. 6), but it is still significantly higher than the present-day value of ~27 mW/m² (Duchkov and Sokolova 1997). Adopting different cut-off thresholds at high and low P – T did not result in significant modification of the calculated geotherm. The combination of lithosphere thickness and geothermal gradient indicates a large ‘diamond window’ beneath Novinka, extending from ca. 110 to over 200 km depth in the middle Paleozoic (344–361 Ma).

Comparison with thermobarometric data for the nearby, broadly coeval (342–360 Ma; Davis et al. 1980) Daldyn kimberlite field (Figs. 6c–e) is hampered by the recognized temperature gap between ca. 900 and 1200 °C in P – T estimates for xenoliths from Udachnaya (Doucet et al. 2013), which reduces the robustness of geotherm fitting, and by non-optimized analytical procedures in the literature data.

Additional ambiguity derives from minor inconsistencies between estimates obtained using different thermobarometer pairs (cf. Doucet et al. 2013). If the same single-clinopyroxene thermobarometers are used for both data sets, the P – T data for Udachnaya appear to be broadly consistent with the Upper Muna calculated geotherm, although somewhat more scattered at high T (Fig. 6e).

GENERAL IMPLICATIONS ON XENOLITH THERMOBAROMETRY AND GEOTHERM EVALUATION

We have shown that careful compositional screening and high-quality analysis of peridotitic clinopyroxenes from the Novinka kimberlite (Upper Muna field, Yakutia) have allowed to reduce thermobarometric uncertainties and to make a good assessment of the thermal state of the lithospheric mantle at the time of kimberlite eruption. It is worth noting, however, that EMP analytical conditions employed in studies of garnet peridotites or diamond inclusions are often not optimized for reliable thermobarometry. Moreover, in many cases, the analytical conditions are not reported or only partial documentation is given. Of twenty-two published papers in which the Cr-in-Cpx barometer is applied and documentation of EMP analytical conditions is provided, twenty used relatively low beam currents (≤ 20 nA) and/or low counting times (≤ 20 s for peak) (e.g., Wang and Gasparik 2001; Menzies et al. 2004; Donnelly et al. 2007; Faryad et al. 2009; Nimis et al. 2009; Doucet et al. 2013; Chen et al. 2014). This casts doubts on the reliability of many existing single-clinopyroxene thermobarometric data and demands proper evaluation of propagation of analytical errors on P estimates.

Although analytical uncertainties will obviously depend not only on the adopted analytical conditions but also on the performance of the equipment and quality of the standardization routines, simplified thresholds based on compositional parameters reported in Table A2 can be used in common practice to define the most appropriate analytical conditions for thermobarometric applications or to help select the most reliable analyses from published datasets. If low beam current and short counting times are used (e.g., 15 nA, 10 s peak, 10 s background), the safety threshold of $a_{\text{Cr}}/\text{Cr\#} > 0.024$ apfu would cut off 19% of the 764 records in the mantle xenolith database of Nimis and Grütter (2010) and

46% of reported clinopyroxene inclusions in peridotitic and websteritic diamonds (cf. Stachel and Harris 2008). Using higher beam current and longer counting times (e.g., 40 nA, 40 s peak, 40 s background) the threshold may decrease to 0.011 apfu, thus cutting off only 4% of the xenoliths and 15% of the inclusions. The $Cr\#$ threshold of 0.1 proposed here cuts off further 5% of the xenoliths (mostly pyroxenites) and 17% of the inclusions (almost all from websteritic diamonds). Note that the $a_{Cr}/Cr\#$ ratio decreases with increasing P/T ratio (Fig. 7). Therefore, clinopyroxenes with compositions that are the most sensitive to propagation of analytical errors on estimated P (i.e., those with the lowest $a_{Cr}/Cr\#$) are those equilibrated under conditions corresponding to the highest P/T ratios. This indicates that clinopyroxene geotherms will tend to be less precise for cold cratonic mantle sections if EMP analyses are not of sufficient quality.

The effect of poor-quality analyses will tend to average out when a large population of chromian diopsides from a certain locality is used. Therefore, definition of mantle thermal state and diamond potential using the sample selection and analytical strategies proposed here may show only marginal improvement with respect to previously proposed protocols (cf. Grütter 2009). Nonetheless, the proportion of ‘accepted’ samples can be increased, the precision of individual P – T estimates can be improved, and ‘unsafe’ compositions are more effectively recognized (Fig. 5). This represents an advantage when the available population of clinopyroxene data is restricted for some reason (e.g. inclusions in diamonds), or when a detailed comparison between individual P – T estimates is required.

It should be emphasized that high-quality analyses *and* appropriate compositional screening will considerably reduce scatter of P – T estimates, but they will not eliminate systematic deviations of Cr-in-Cpx pressures due to inconsistencies in its calibration. In fact, the progressive negative deviation of Cr-in-Cpx P estimates relative to orthopyroxene–garnet P estimates at $P > 4.5$ GPa (Fig. 4) confirms the tendency of the Cr-in-Cpx barometer to underestimate at high P (by ca. 1 GPa at 7 GPa), which was previously observed against a limited set of experimental data (cf. Nimis 2002). Moreover, a slight positive deviation of the Cr-in-Cpx pressures (<0.5 GPa on average) is observed at P around 3 GPa

(Fig. 4), which partly confirms observations by Grütter and Moore (2003) and Grütter (2009). It is unclear if this small discrepancy at moderate P is due to inaccuracy of the Cr-in-Cpx barometer, of the orthopyroxene–garnet barometer, or of both. Owing to these systematic deviations, mantle palaeogeotherms calculated on the basis of single-Cpx thermobarometry will tend to show slightly different shapes than those based on orthopyroxene–garnet barometry. The most important discrepancies will affect the deepest portion of the lithosphere, where clinopyroxene geotherms will tend to show slightly overestimated T/P gradients. As discussed by Nimis (2002), this drawback will not hamper recognition of samples coming from the diamond window.

Acknowledgments

The present work is part of LZ's PhD research program at the University of Padova (Italy). The authors are indebted to G. Pearson, L. Franz and to late J. Boyd for supplying materials for the present study, and to R. Carampin (IGG-CNR, Padova) for his invaluable help during analytical sessions. H. Grütter and T. Stachel are thanked for sharing their compilations of xenolith and diamond inclusion data. S. Klemme is thanked for precious suggestions. Formal reviews by H. Grütter and an anonymous referee pointed out some important flaws in our original manuscript and helped us significantly improve this paper. PN acknowledges support by ERC Starting Grant 307322 (project INDIMEDEA). LZ acknowledges support by Fondazione Cassa di Risparmio di Padova e Rovigo – “Progetto Dottorati di Ricerca 2009”. We thank A.V. Sobolev for the given opportunity to perform analytical procedures at the EPMA laboratory of the Max Planck Institute for Chemistry. VM and DK were supported by Russian Foundation for Basic Research (grant No. 16-05-01052). VM was supported by state assignment project No. 0330-2016-0006 and by Russian Science Foundation (grant No. 16-17-10067).

REFERENCES

- Agashev, A.M., Pokhilenko, N.P., Tolstov, A.V., Polyanichko, V.V., Malkovets, V.G., Sobolev, N.V., 2004. New age data on kimberlites from the Yakutian diamondiferous province. *Doklady Akademii Nauk SSSR, Earth Science Section* 399, 1142–1145.
- Agashev, A.M., Ionov, D.A., Pokhilenko, N.P., Golovin, A.V., Cherepanova, Y., and Sharygin, I.S. (2013) Metasomatism in lithospheric mantle roots: Constraints from whole-rock and mineral chemical composition of deformed peridotite xenoliths from kimberlite pipe Udachnaya. *Lithos*, 160-161, 201-215.
- Ashchepkov, I.V., Pokhilenko, N.P., Vladykin, N.V., Logvinova, A.M., Afanasiev, V.P., Pokhilenko, L.N., Kuligin, S.S., Malygina, E.V., Alyмова, N.A., Kostrovitsky, S.I., Rotman, A.Y., Mityukhin, S.I., Karpenko, M.A., Stegnitsky, Y.B., and Khemel'nikova, O.S. (2010) Structure and evolution of the lithospheric mantle beneath Siberian craton, thermobarometric study. *Tectonophysics*, 485, 17-41.
- Ashchepkov, I.V., Pokhilenko, N.P., Vladykin, N.V., Rotman, A.Y., and Afanasiev, V.P. (2008) Reconstruction of mantle sections beneath Yakutian kimberlite pipes using monomineral thermobarometry. *Geological Society Special Publications*, 293, 335-352.
- Boyd, F.R. (1973) A pyroxene geotherm. *Geochimica et Cosmochimica Acta*, 37, 2533-2546.
- Boyd, F.R. (1984) A Siberian geotherm based on lherzolite xenoliths from the Udachnaya kimberlite, U.S.S.R. *Geology*, 12, 528-530.
- Boyd, F.R., Pokhilenko, N.P., Pearson, D.G., Mertzman, S.A., Sobolev, N.V., and Finger, L.W. (1997) Composition of the Siberian cratonic mantle: evidence from Udachnaya peridotite xenoliths. *Contributions to Mineralogy and Petrology*, 128, 228-246.
- Canil, D. (1999) The Ni-in-garnet geothermometer: calibration at natural abundances. *Contributions to Mineralogy and Petrology*, 136, 240-246.

- Carswell, D.A. (1991) The garnet–orthopyroxene Al barometer: problematic application to natural garnet lherzolite assemblages. *Mineralogical Magazine*, 55, 19-31.
- Chen, M.M, Tian, W., Suzuki, K., Tejada, M.L.G., Liu, F.L., Senda, R., Wei, C.J., Chen, B., and Chu, Z.Y. (2014) Peridotite and pyroxenite xenoliths from Tarim, NW China: Evidences for melt depletion and mantle refertilization in the mantle source region of the Tarim flood basalt. *Lithos*, 204, 97-111.
- Cookenboo, H.O., and Grütter, H.S. (2010) Mantle-derived indicator mineral compositions as applied to diamond exploration. *Geochemistry: Exploration, Environment, Analysis*, 10, 81-95.
- Davis, G.L., Sobolev, N.V., and Khar’kiv, A.D. (1980) New data on the age of Yakutian kimberlites obtained by the uranium–lead method on zircons (in Russian). *Doklady AN SSSR*, 254, 175-180.
- Day, H.W. (2012) A revised diamond-graphite transition curve. *American Mineralogist*, 97, 52-62.
- Donnelly, C.L., Stachel, T., Creighton, S., Muehlenbachs, K., and Whiteford, S. (2007) Diamonds and their mineral inclusions from the A154 South pipe, Diavik Diamond Mine, Northwest territories, Canada. *Lithos*, 98, 160-176.
- Doucet, L.S., Ionov, D.A., and Golovin, A.V. (2013) The origin of coarse garnet peridotites in cratonic lithosphere: new data on xenoliths from the Udachnaya kimberlite, central Siberia. *Contributions to Mineralogy and Petrology*, 165, 1225-1242.
- Duchkov, A.D., and Sokolova, L.S. (1997) Thermal pattern of the lithosphere of the Siberian Platform (in Russian). *Geologiya i Geofizika*, 38, 494-503.
- Eaton, D.W., Darbyshire, F., Evans, R.L., Grütter, H., Jones, A.G., and Yuan, X. (2009) The elusive lithosphere–asthenosphere boundary (LAB) beneath cratons. *Lithos*, 109, 1-22.
- Faryad, S.W., Dolejš, D., and Machek, M. (2009) Garnet exsolution in pyroxene from clinopyroxenites in the Moldanubian zone: constraining the early pre-convergence history of ultramafic rocks in the Variscan orogen. *Journal of Metamorphic Geology*, 27, 655-671.

- Goncharov, A.G., Ionov, D.A., and Doucet, L.S. (2012) Thermal state, oxygen fugacity and C-O-H fluid speciation in cratonic lithospheric mantle: new data on peridotite xenoliths from the Udachnaya kimberlite, Siberia. *Earth and Planetary Science Letters*, 357-358, 99-110.
- Griffin, W.L., Fisher, N.I., Friedman, J.H., O'Reilly, S.Y., and Ryan, C.G. (2002) Cr-pyrope garnets in the lithospheric mantle. II. Compositional populations and their distribution in time and space. *Geochemistry, Geophysics, Geosystems*, 3, 1073, doi:10.1029/2002GC000298.
- Griffin, W.L., Kaminsky, F.V., Ryan, C.G., O'Reilly, S.Y., Win, T.T., and Ilupin, I.P. (1996) Thermal state and composition of the lithospheric mantle beneath the Daldyn kimberlite field, Yakutia. *Tectonophysics*, 262, 19-33.
- Griffin, W.L., O'Reilly, S.Y., Doyle, B.J., Pearson, N.J., Coopersmith, H., Kivi, K., Malkovets, V., and Pokhilenko, N. (2004) Lithosphere mapping beneath the North American plate. *Lithos*, 77, 873-922.
- Griffin, W.L., Ryan, C.G., Kaminsky, F.V., O'Reilly, S.Y., Natapov, L.M., Win, T.T., Kinny, P.D., and Ilupin, I.P. (1999) The Siberian lithosphere traverse. Mantle terranes and the assembly of the Siberian craton. *Tectonophysics*, 310, 1-35.
- Grütter, H., Latti, D., and Menzies, A.H. (2006) Cr-saturation arrays in concentrate garnet compositions from kimberlite and their use in mantle barometry. *Journal of Petrology*, 47, 801-820.
- Grütter, H., and Moore, R. (2003) Pyroxene geotherms revisited - an empirical approach based on Canadian xenoliths. *Extended Abstract 8th International Kimberlite Conference* no. 272.
- Grütter, H.S. (2009) Pyroxene xenocryst geotherms: techniques and application. *Lithos*, 112, 1167-1178.
- Grütter, H.S., and Tuer, J. (2009) Constraints on deep mantle tenor of Sarfartoq-area kimberlites (Greenland), based on modern thermobarometry of mantle-derived xenocrysts. *Lithos*, 112, 124-129.
- Hasterok, D., and Chapman, D.S. (2011) Heat production and geotherms for the continental lithosphere. *Earth and Planetary Science Letters*, 307, 59-70.

- Ionov, D.A., Doucet, L.S., and Ashchepkov, I.V. (2010) Composition of the lithospheric mantle in the Siberian craton: new constraints from fresh peridotites in the Udachnaya-East kimberlite. *Journal of Petrology*, 51, 2177-2210.
- Janney, P.E., Shirey, S.B., Carlson, R.W., Pearson, D.G., Bell, D.R., Le Roex, A.P., Ishikawa, A., Nixon, P.H., and Boyd, F.R. (2010) Age, composition and thermal characteristics of South African off-craton mantle lithosphere: Evidence for a multi-stage history. *Journal of Petrology*, 51, 1849-1890.
- Kopylova, M.G., Russell, J.K., and Cookenboo, H. (1998) Upper-mantle stratigraphy of the Slave craton, Canada: Insights into a new kimberlite province. *Geology*, 26, 315-318.
- Lazarov, M., Woodland, A.B., and Brey, G.P. (2009) Thermal state and redox conditions of the Kaapvaal mantle: A study of xenoliths from the Finsch mine, South Africa. *Lithos*, 112S, 913-923.
- Lehtonen, M., O'Brien, H., Peltonen, P., Kukkonen, I., Ustinov, V., and Verzhak, V. (2009) Mantle xenocrysts from the Arkhangelskaya kimberlite (Lomonosov mine, NW Russia): Constraints on the composition and thermal state of the diamondiferous lithospheric mantle. *Lithos*, 112, 924-933.
- Lepekhina, E.N., Rotman, A.Y., Antonov, A.V., and Sergeev, S.A. (2008a) SHRIMP U-Pb zircon of Yakutian kimberlites pipes. Extended Abstract 9th International Kimberlite Conference, no. 9IKC-A-00354.
- Lepekhina, E.N., Rotman, A.Y., Antonov, A.V., and Sergeev, S.A. (2008b) SHRIMP U-Pb perovskite from kimberlites of the Siberian platform (Verhnemunskoe and Alakite-Marhinskoe fields). Extended Abstract 9th International Kimberlite Conference, no. 9IKC-A-00353.
- Levchenkov., O.A., Gaidamako, I.M., Levskii, L.K., Komarov, A.N., Yakovleva, S.Z., Rizvanova N.G., and Makeev, A.F. (2005) U-Pb age of zircon from the Mir and 325 Let Yakutii Pipes. *Doklady Earth Science*, 400, 99-101.
- Malkovets, V.G., Griffin, W.L., O'Reilly, S.Y., and Wood, B.J., 2007. Diamond, subcalcic garnet, and mantle metasomatism: kimberlite sampling patterns define the link. *Geology* 35 (4), 339–342.

- Manakov, A. (2002) Moho depth beneath the Siberian kimberlite fields. Mirny, Russia. 352 p. PhD thesis.
- Mather, K.A., Pearson, D.G., McKenzie, D., Kjarsgaard, B.A., and Priestley, K. (2011) Constraints on the depth and thermal history of cratonic lithosphere from peridotite xenoliths, xenocrysts and seismology. *Lithos*, 125, 729-742.
- McKenzie, D., and Bickle, M.J. (1988) The volume and composition of melt generated by extension of the lithosphere. *Journal of Petrology*, 29, 625-679.
- McKenzie, D., Jackson, J., and Priestley, K. (2005) Thermal structure of oceanic and continental lithosphere. *Earth and Planetary Science Letters*, 233, 337-349.
- Menzies, A., Westerlund, K., Grütter, H., Gurney, J., Carlson, J., Fung, A., and Nowicki, T. (2004) Peridotitic mantle xenoliths from kimberlites on the Ekati Diamond Mine property, N.W.T., Canada: major element compositions and implications for the lithosphere beneath the central Slave craton. *Lithos*, 77, 395-412. *Chemical Geology*, 368, 97-103.
- Nickel, K.G., and Green, D.H. (1985) Empirical geothermobarometry for garnet peridotites and implications for the nature of the lithosphere, kimberlites and diamonds. *Earth and Planetary Science Letters*, 73, 158-170.
- Nielsen, C.H., and Sigurdsson, H. (1981) Quantitative methods for electron microprobe analysis of sodium in natural and synthetic glasses. *American Mineralogist*, 66, 547-552.
- Nimis, P. (1998) Evaluation of diamond potential from the composition of peridotitic chromian diopside. *European Journal of Mineralogy*, 10, 505-519.
- Nimis, P. (2002) The pressures and temperatures of formation of diamond based on thermobarometry of chromian diopside inclusions. *Canadian Mineralogist*, 40, 871-884.
- Nimis, P., and Grütter, H. (2010) Internally consistent geothermometers for garnet peridotites and pyroxenites. *Contributions to Mineralogy and Petrology*, 159, 411-427.

- Nimis, P., and Taylor, W.R. (2000) Single-clinopyroxene thermobarometry for garnet peridotites. Part I. Calibration and testing of a Cr-in-Cpx barometer and an enstatite-in-Cpx thermometer. *Contributions to Mineralogy and Petrology*, 139, 541-554.
- Nimis, P., Zanetti, A., Dencker, I., and Sobolev, N.V. (2009) Major and trace element composition of chromian diopsides from the Zagadochnaya kimberlite (Yakutia, Russia): Metasomatic processes, thermobarometry and diamond potential. *Lithos*, 112, 397-412.
- O'Reilly, S.Y., and Griffin, W.L. (1985) A xenolith-derived geotherm for southeastern Australia and its geological implications. *Tectonophysics*, 111, 41-63.
- Osako, M., Ito, E., and Yoneda, A. (2004) Simultaneous measurements of thermal conductivity and thermal diffusivity for garnet and olivine under high pressure. *Physics of the Earth and Planetary Interiors*, 143, 311-320.
- Pokhilenko, N.P., Sobolev, N.V., Boyd, F.R., Pearson, D.G., and Shimizu, N. (1993) Megacrystalline pyrope peridotites in the lithosphere of the Siberian platform: Mineralogy, geochemical peculiarities and the problem of their origin. *Russian Geology and Geophysics*, 34, 56-67.
- Pokhilenko, N.P., Sobolev, N.V., Kuligin, S.S., and Shimizu, N. (1999) Peculiarities of distribution of pyroxenite paragenesis garnets in Yakutian kimberlites and some aspects of the evolution of the Siberian craton lithospheric mantle. In: J.J. Gurney, J.L. Gurney, M.D. Pascoe, S.H. Richardson (Eds.), *Proceedings of the 7th International Kimberlite Conference*, vol.2. p. 689-698.
- Pollack, H.N., and Chapman, D.S. (1977) On the regional variations of heat flow, geotherms and lithospheric thickness. *Tectonophysics*, 38, 279-296.
- Potts, P.J., Tindle A.G., and Isaacs, M.C. (1983) On the precision of electron microprobe data: a new test for the homogeneity of mineral standards. *American Mineralogist*, 68, 1237-1242.
- Putirka, K.D. (2008) Thermometers and barometers for volcanic systems. *Reviews in Mineralogy and Geochemistry*, 69, 61-120.

- Ramsay, R.R., and Tompkins, L.A. (1994) The geology, heavy mineral concentrate mineralogy, and diamond prospectivity of the Boa Esperança and Cana Verde pipes, Corrego D'anta, Minas Gerais, Brazil. In: H.O.A. Meyer, O.H. Leonardos (Eds.), *Kimberlites, Related Rocks and Mantle Xenoliths CPRM, Special Publications*, p. 329-345, Brasilia, Brazil.
- Read, G.H., and Janse, A.J.A. (2009) Diamonds: Exploration, mines and marketing. *Lithos*, 112, 1-9.
- Read, G.H., Grütter, H., Winter, S., Luckman, N., Gaunt, F., and Thomsen, F. (2004) Stratigraphic relations, kimberlite emplacement and lithospheric thermal evolution, Quirico' Basin, Minas Gerais State, Brazil. *Lithos*, 77, 803–818.
- Rosen, O.M., Soloviev, A.V., and Zhuravlev, D.Z. (2009) Thermal evolution of the northeastern Siberian Platform in the light of apatite fission-track dating of the Deep Drill Core. *Izvestiya, Physics of the Solid Earth*, 45, 914-931.
- Ryan, C.G., Griffin, W.L., and Pearson, N.J. (1996) Garnet geotherms: pressure–temperature data from Cr-pyropes garnet xenocrysts in volcanic rocks. *Journal of Geophysical Research*, 101, 5611-5625.
- Shimizu, N., Pokhilenko, N.P., Boyd, F.R., and Pearson, D.G. (1997) Geochemical characteristics of mantle xenoliths from the Udachnaya kimberlite pipe. *Proceedings of the 6th International Kimberlite Conference vol.1*, p. 205-217.
- Shirey, S.B., Cartigny, P., Frost, D.J., Keshav, S., Nestola, F., Nimis, P., Pearson, D.G., Sobolev, N.V., and Walter, M.J. (2013) Diamonds and the geology of mantle carbon. *Reviews in Mineralogy and Geochemistry*, 75, 355-421.
- Smith, D. (1999) Temperatures and pressures of mineral equilibration in peridotite xenoliths: review, discussion, and implications. In: Y. Fei, C.M. Bertka, B.O. Mysen (Eds.), *Mantle petrology: field observations and high pressure experimentation: a tribute to Francis R. (Joe) Boyd*, vol 6. *Geochemical Society Special Publications*, p. 171-188.
- Stachel, T., and Harris, J.W. (2008) The origin of cratonic diamonds – constraints from mineral inclusions. *Ore Geology Review*, 34, 5-32.

- Sun, J., Liu, C.Z., Tappe, S., Kostrovitsky, S.I., Wu, F.Y., Yakovlev, D., Yang, Y.-H., and Yang, J.H. (2014) Repeated kimberlite magmatism beneath Yakutia and its relationship to Siberian flood volcanism: insights from in situ U–Pb and Sr–Nd perovskite isotope analysis. *Earth Planet. Sci. Lett.* 404, 283-295.
- Taylor, W.R. (1998) An experimental test of some geothermometer and geobarometer formulations for upper mantle peridotites with application to the thermobarometry of fertile lherzolite and garnet websterite. *Neues Jahrbuch für Mineralogie, Abhandlungen*, 172, 381-408.
- Wang, W., and Gasparik, T. (2001) Metasomatic clinopyroxene inclusions in diamonds from the Liaoning province, China. *Geochimica et Cosmochimica Acta*, 65, 611-62.
- Zozulya, D.R., O'Brien, H., Peltonen, P., and Lehtonen, M. (2009) Thermobarometry of mantle-derived garnets and pyroxenes of Kola region (NW Russia): Lithosphere composition, thermal regime and diamond prospectivity. *Bulletin of the Geological Society of Finland*, 81, 143-15.

APPENDIX. PROPAGATION OF ANALYTICAL ERRORS IN SINGLE-CLINOPYROXENE GEOBAROMETRY

The Cr-in-Cpx barometer (Nimis and Taylor, 2000) is expressed as

$$P(\text{kbar}) = -\frac{T(\text{K})}{126.9} \cdot \ln a_{\text{Cr}} + 15.483 \cdot \ln \left(\frac{\text{Cr}\#}{T(\text{K})} \right) + \frac{T(\text{K})}{71.38} + 107.8 \quad (1)$$

where $a_{\text{Cr}} = \text{Cr} - 0.81 \cdot \text{Na} \cdot \text{Cr}\#$ and $\text{Cr}\# = \text{Cr}/(\text{Cr} + \text{Al})$, with elements in apfu. Although the effect of K on Cpx barometry was unknown, Nimis and Taylor (2000) suggested that any K should be added to Na in P calculations. Assuming random error sources, the uncertainties on pressure estimates can be expressed with a normal error propagation function, i.e.,

$$\sigma P = \sqrt{\left(\frac{\partial P}{\partial \text{Cr}} \cdot \sigma \text{Cr} \right)^2 + \left(\frac{\partial P}{\partial \text{Al}} \cdot \sigma \text{Al} \right)^2 + \left(\frac{\partial P}{\partial \text{Na}} \cdot \sigma \text{Na} \right)^2 + \left(\frac{\partial P}{\partial T} \cdot \sigma T \right)^2} \quad (2)$$

Calculation of σP requires knowledge of analytical uncertainties on Cr, Al, Na and T . The influence of analytical uncertainties on the very minor K contents can safely be neglected. Uncertainties on T estimates can be derived from reproducibility of temperatures of experiments in two-pyroxene-bearing assemblages using the enstatite-in-Cpx thermometer (± 30 – 40°C ; Nimis and Taylor 2000). Accurate evaluation of EMP uncertainties is not straightforward, because analytical errors primarily depend on both the absolute element concentrations and on the analytical conditions adopted for the analysis.

In this appendix, we will investigate the effect of EMP uncertainties on pressure estimates for compositionally diverse clinopyroxenes. As a first step, we will evaluate the analytical errors for different analytical conditions and for a specific set of clinopyroxene compositions through repeat EMP measurements on compositionally homogeneous areas of selected cpx grains, and evaluate the propagated uncertainties on P estimates by calculating P for each analysis. We then apply the error propagation function (Equation 2) to a great variety of natural clinopyroxene compositions, assuming model analytical uncertainties derived from the first test.

First step: evaluation of uncertainties vs. analytical conditions

We selected seven clinopyroxenes having a_{Cr} between 0.0016 and 0.0188 apfu, characterized by various proportions of Al, Cr and Na, and equilibrated in a wide range of P – T conditions (Table A1). Appropriate compositions were found in four clinopyroxene xenocrysts from the Novinka kimberlite (this study) and three clinopyroxenes from three well-studied garnet peridotites. Description of the garnet peridotite samples is reported in Supplementary Material S3.

Chemical analyses were carried out with a CAMECA SX-50 electron microprobe (IGG–CNR, Padua, Italy), equipped with four wavelength-dispersive spectrometers using one LIF, one PET, and two TAP crystals. Natural and synthetic minerals (diopside for Ca and Si, albite for Na, orthoclase for K, and pure Al, Mg, Cr, Fe, and Mn-Ti oxides) were used as standards. X-ray counts were converted into weight percent oxides by using the CAMECA-PAP program. Each clinopyroxene grain/portion was first analyzed for all elements adopting routine analytical condition, i.e., 1 μm electron beam, 20 kV accelerating voltage, 15 nA beam current, and a counting time of 10 s for peak and 10 s for background (i.e., 5 s on each side of the peak). The most mobile elements were always analyzed first in order to minimize their migration under the electron beam. The sequence of element analyses on each spectrometer was thus as follows: Fe, Mn, Cr (LIF); Si, Al (TAP); Na, Mg (TAP); K, Ca, Ti (PET). This preliminary investigation allowed us to select compositionally homogeneous areas and provided us with average compositions to be used for calculation of matrix effects in subsequent analytical sessions and for preliminary thermobarometry (Table A1).

The same clinopyroxenes were then analyzed again for Al, Cr and Na using increasing beam currents and counting times (Table A2). Five analytical sessions were carried out, during which 15 individual point analyses were acquired on the same, homogeneous areas of each clinopyroxene. The analyses were carried out on a grid of 3 x 5 analytical spots (maximum side 20 μm). To limit element migration under the electron beam, before each session the grid was translated by 3–4 μm , within the previously defined homogeneous areas. Calcium was also measured on the same spots as a further check for compositional homogeneity. The four elements were analyzed simultaneously with the four

independent spectrometers. Observed absolute variations in CaO weight percentages between individual point analyses were always ≤ 0.5 wt%. No systematic variations in X-ray counts for Na were observed using different beam currents (i.e., 15 nA and 40 nA), not even after a 300-s count period, implying that Na did not significantly mobilize under the electron beam during our analyses (cf. Nielsen and Sigurdsson 1981). No analyses for which any measured concentration departed by more than 3 standard deviations from the mean were obtained. The average compositions obtained during the five test sessions on each selected clinopyroxene are reported in Table A3.

For each point analysis, $Cr\#$, a_{Cr} and Cr-in-Cpx pressure were calculated. Pressures were calculated using fixed input temperature values, which were obtained by applying the enstatite-in-Cpx thermometer, at P given by the Cr-in-Cpx barometer, on the compositions derived from the preliminary analyses of the samples (Table A1). Statistical parameters (mean values, standard deviations, and quantiles) for all relevant variables are reported in Table A3 and illustrated in Figure A1.

The relative uncertainties on the measured Al, Cr and Na concentrations decrease smoothly with increasing beam current, counting times, and element abundances (Table A3). This allowed us to model analytical uncertainties as functions of clinopyroxene composition for each set of analytical conditions (Table A4). The standard deviations on P estimates drastically change with changing analytical conditions (σ as high as 1.1 GPa using the lowest beam current and counting times) and clinopyroxene composition (Table A3 and Fig. A1).

The relationships between P uncertainties and composition can be explained considering the topology of the Cr-in-Cpx barometer expression (Equation 1). In equation (1), P is related to a_{Cr} and $Cr\#$ through two logarithmic functions. This enhances error propagation with decreasing a_{Cr} and $Cr\#$. Owing to its greater weight in the equation, the effect of the a_{Cr} logarithmic term tends to be dominant in terms of error propagation. This accounts well for the larger P uncertainties obtained for the clinopyroxene Nov-42 ($a_{Cr} = 0.0016$ apfu) with respect to clinopyroxene Uv61/91 ($a_{Cr} = 0.0081$ apfu), in spite of their similar a_{Cr} uncertainties (Table A3). It also explains the progressively larger, non-

systematic deviations from orthopyroxene–garnet pressures at lower a_{Cr} (Figs. 2 and 4). Moreover, because of the logarithmic relation, the distribution of propagated errors due to a_{Cr} uncertainties tends to be skewed towards the positive side.

Whereas the effect of the $Cr\#$ logarithmic term on error propagation is marginal, $Cr\#$ has a major effect on the uncertainties of the a_{Cr} parameter. In particular, a higher $Cr\#$ will enhance propagation of Na uncertainties on a_{Cr} and, therefore, on P . This explains the lower P uncertainties (and their less pronounced variations between different analytical sessions) obtained for clinopyroxene Nov-80, which is characterized by low a_{Cr} (0.003 apfu) and low $Cr\#$ (0.13), compared with those obtained for compositions with higher $Cr\#$ values (Table A3 and Fig. A1).

Second step: P uncertainties in the natural clinopyroxene compositional space and optimum analytical conditions for clinopyroxene barometry

The above test showed that the effect of analytical errors on the precision and accuracy of the calculated pressure strongly increases with decreasing a_{Cr} and with increasing $Cr\#$. For any clinopyroxene composition, minimum analytical conditions should be defined for which analytical errors propagate acceptable errors on pressure estimates. For this purpose, a more extended test on a comprehensive set of clinopyroxene compositions is needed. We have used the database of well-equilibrated xenoliths of Nimis and Grütter (2010) as our test material. Temperatures for each xenolith were calculated using the thermometer of Taylor (1998) at P given by the orthopyroxene–garnet barometer of Nickel and Green (1985; with modifications by Carswell 1991, his equations E6 and E9, assuming no ferric iron). The T uncertainty was fixed at 40 °C (cf. Nimis and Taylor 2000). Uncertainties on clinopyroxene Cr, Al and Na analyses were calculated for each xenolith for five combinations of analytical conditions, taking into account the results of our previous analytical test (Table A4). Uncertainties on Cr-in-Cpx pressures were then calculated by normal error propagation of the five resulting sets of analytical uncertainties (Equation 2).

As expected, the calculated uncertainties increase with decreasing a_{Cr} and increasing $Cr\#$ values (Fig. 3), reaching 1.8 GPa when a_{Cr} is <0.002 apfu and the lowest current and counting times are assumed. These results can be used to determine an approximate compositional threshold below which pressure estimates become too sensitive to analytical errors. We consider a propagated uncertainty of ± 0.25 GPa on the calculated P , including the effect of both analytical and thermometric errors, to be a reasonable limit. Taking into account the standard error of estimate of the barometer calibration (± 0.23 GPa), this limit should ensure an overall uncertainty smaller than ± 0.4 GPa. We found that simplified thresholds based on the $a_{Cr}/Cr\#$ ratio (Table A2) permit discrimination of compositions for which P uncertainties are acceptable to within a 95% confidence limit.

Figure 1. Sketch tectonic map of the Siberian platform with major kimberlite fields. Terranes are outlined by dashed curves and are named in *italic*. Modified after Griffin et al. (1999).

Figure 2. Discrepancies between the Cr-in-Cpx barometer (Nimis and Taylor 2000; P_{NT00}) and the orthopyroxene-garnet barometer (P_{Ca91} ; Nickel and Green 1985, as modified by Carswell 1991) vs. the clinopyroxene parameter a_{Cr} . Clinopyroxene compositions are from the compilation of well-equilibrated garnet peridotite and pyroxenite xenoliths of Nimis and Grütter (2010). In **(a)** the entire dataset has been included, while in **(b)** only clinopyroxene plotting in the high-Al field of Nimis (1998) [$Al_2O_3 \geq 0.7$ wt%; $Al_2O_3 \geq 12.175 - 0.6375 \cdot MgO$ wt%] and having $Cr\#$ between 0.06 and 0.50 (Grütter, 2009) have been plotted. The overall shift of high- P clinopyroxenes towards negative values can be ascribed to the known underestimation of P_{NT00} at high P (cf. Nimis 2002).

Figure 3. Calculated P uncertainties (σ) vs. a_{Cr} for clinopyroxenes from well-equilibrated garnet peridotites and pyroxenites (database of Nimis and Grütter 2010). The P uncertainties were calculated from normal propagation of T uncertainties ($\pm 40^\circ C$) and analytical errors derived from equations reported in Table A4 assuming **(a)** the lowest beam current (15 nA) and counting times (10 s peak, 5 + 5 s background) and **(b)** the highest beam current (40 nA) and counting times (40 s peak, 20 + 20 s background).

Figure 4. P estimates using the Cr-in-Cpx barometer (Nimis and Taylor 2000; P_{NT00}) plotted versus P estimates using the orthopyroxene–garnet barometer of Nickel and Green (1985, as modified by Carswell 1991; P_{Ca91}) for **(a)** the entire dataset of well equilibrated garnet peridotites and pyroxenites of Nimis and Grütter (2010) and **(b)** the same dataset excluding samples with calculated Cr-in-Cpx pressure uncertainties greater than ± 0.25 GPa.

Figure 5. Results of single-clinopyroxene thermobarometry (Nimis and Taylor 2000) for the Novinka kimberlite. In **(a)** the accepted analyses have been selected on the basis of the revised protocol for single-clinopyroxene thermobarometry (this work), which takes into account the results of our analytical test (Appendix). For comparison, plot **(b)** shows the results of the filtering protocol of

Grütter (2009) applied on the same initial dataset (97 routine analyses; see text). Dashed curves are classical reference conductive geotherms for different surface heat-flows (mW/m^2) after Pollack and Chapman (1977). The graphite (G) - diamond (D) boundary (solid curve) is after Day (2012).

Figure 6. Model palaeogeotherms calculated using the program FITPLOT (McKenzie et al. 2005). The palaeogeotherm for Novinka are calculated **(a)** using all P - T estimates based on optimized clinopyroxene analyses and **(b)** excluding data plotting above 5.5 GPa. The smaller plots show P - T data for Udachnaya xenoliths, calculated using the geothermometer of Nimis and Taylor (2000; T_{NT00}) in combination with **(c)** the Nickel and Green (1985; P_{NG85}) geobarometer, **(d)** its modification by Carswell (1991; P_{Ca91}), and **(e)** the Cr-in-Cpx geobarometer of Nimis and Taylor (2000; P_{NT00}). Grey symbols in **(e)** indicate clinopyroxenes for which the calculated σ_P is > 0.25 GPa (taking into account the analytical conditions used for the analysis as reported in the source papers). Source mineral compositions for Udachnaya are from Boyd (1984), Pokhilenko et al. (1993), Shimizu et al. (1997), Ionov et al. (2010), Goncharov et al. (2012), and Doucet et al. (2013).

Figure 7. Relationships between P/T gradients, $a_{\text{Cr}}/\text{Cr}\#$ in clinopyroxene, and uncertainties of Cr-in-Cpx pressure propagated from analytical errors. Filled circles are $a_{\text{Cr}}/\text{Cr}\#$ values of the experimental clinopyroxenes used for the calibration of the Cr-in-Cpx barometer (Nimis and Taylor 2000), empty squares are $a_{\text{Cr}}/\text{Cr}\#$ values of natural clinopyroxenes from well-equilibrated peridotites (Nimis and Grütter 2010) and crosses are calculated P uncertainties for the same dataset (see Fig. 3 and text for calculation methods). Natural clinopyroxenes with $\text{Cr}\# < 0.1$, which are considered unsuitable for geobarometry (see text), were excluded from the plot. The approximate correspondence between P/T gradients and steady-state continental geotherms (Pollack and Chapman 1977) is also indicated at the top of the plot. Geobarometry of clinopyroxenes from relatively cold mantle sections ($< 40 \text{ mW/m}^2$) is clearly more sensitive to propagation of analytical errors.

Figure A1. Box-plots of calculated pressures for the test clinopyroxenes analyzed using different operating conditions (cf. Table A2). Median values (thicker vertical lines), interquartile range (boxes), whiskers (dashed lines indicating variability outside the upper and lower quartiles) and individual P estimates for each point analyses (empty circles) are shown. A few analyses of sample Nov-42 resulted in negative values of a_{Cr} and were therefore excluded from calculations.

Figure 1

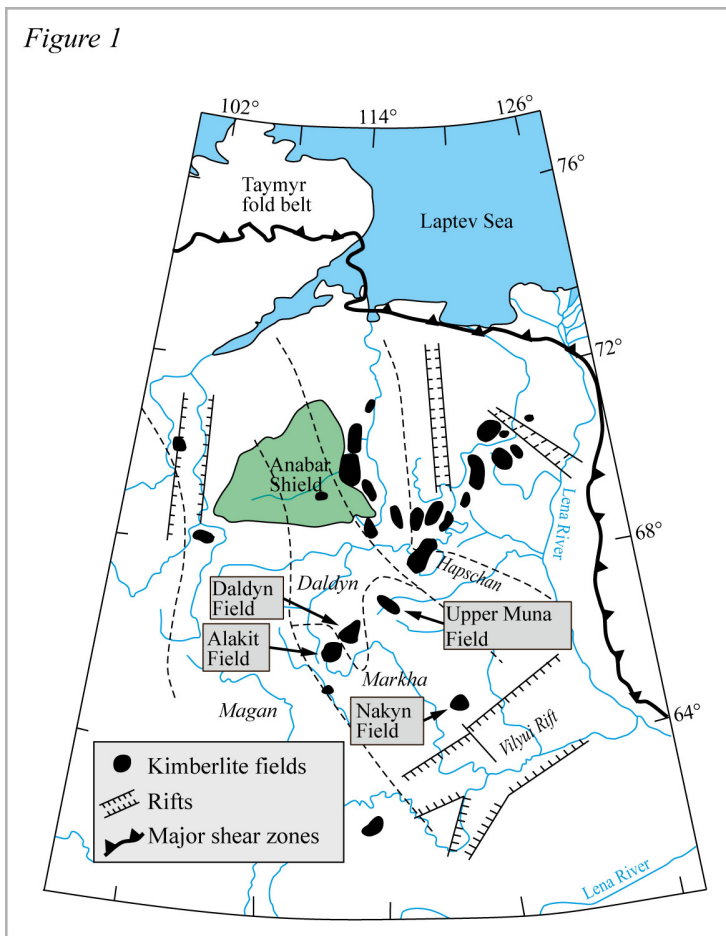


Figure 2

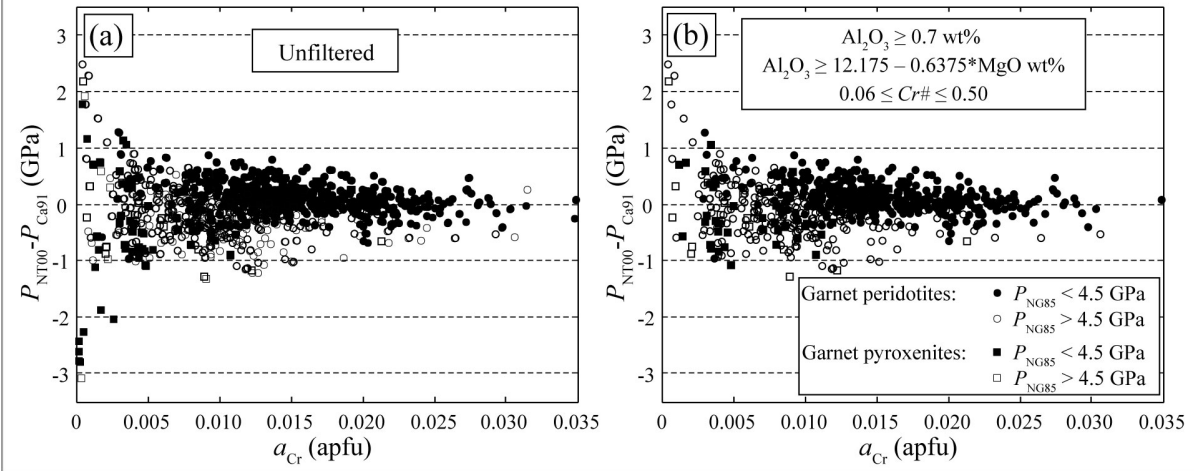


Figure 3

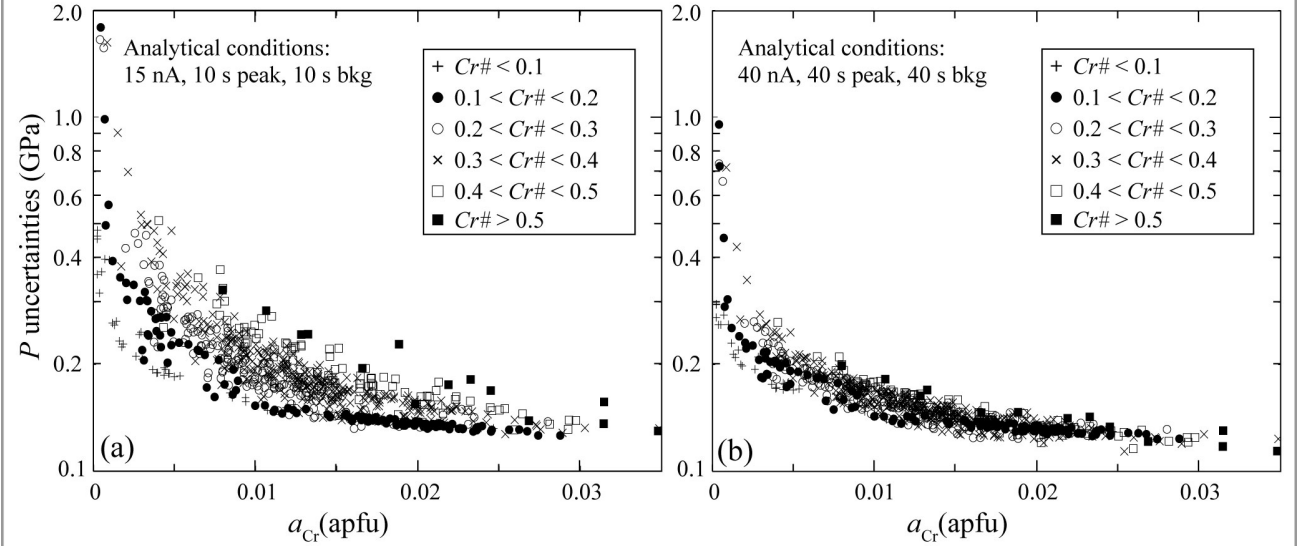


Figure 4

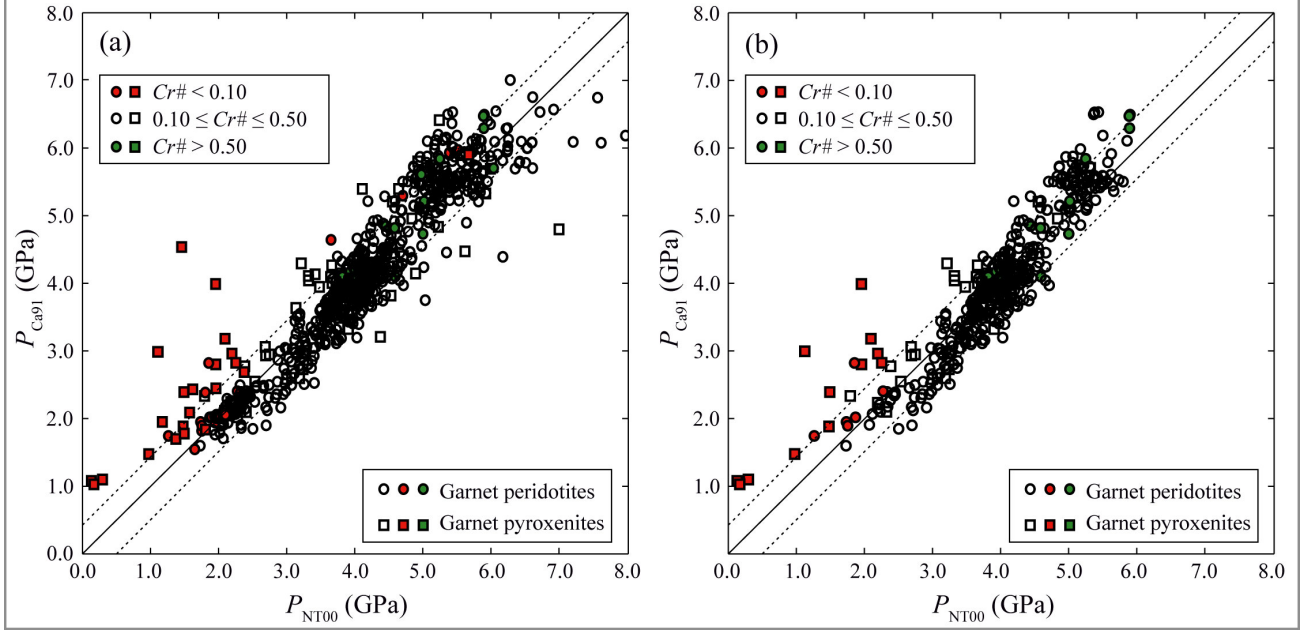


Figure 5

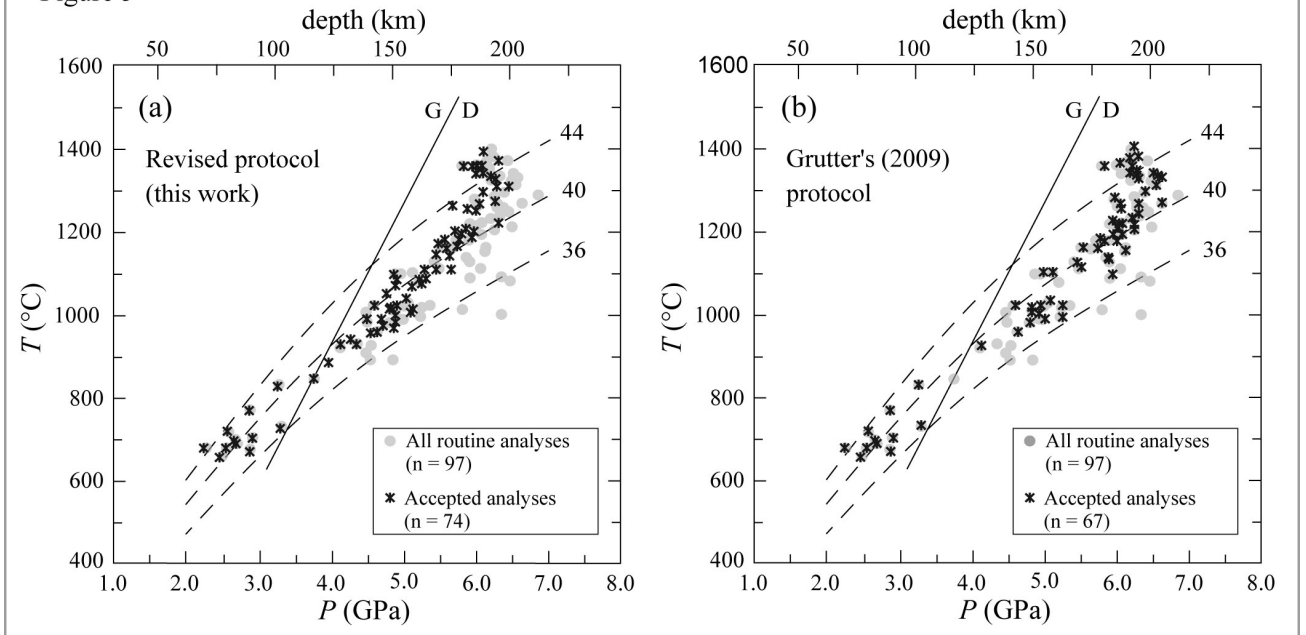


Figure 6

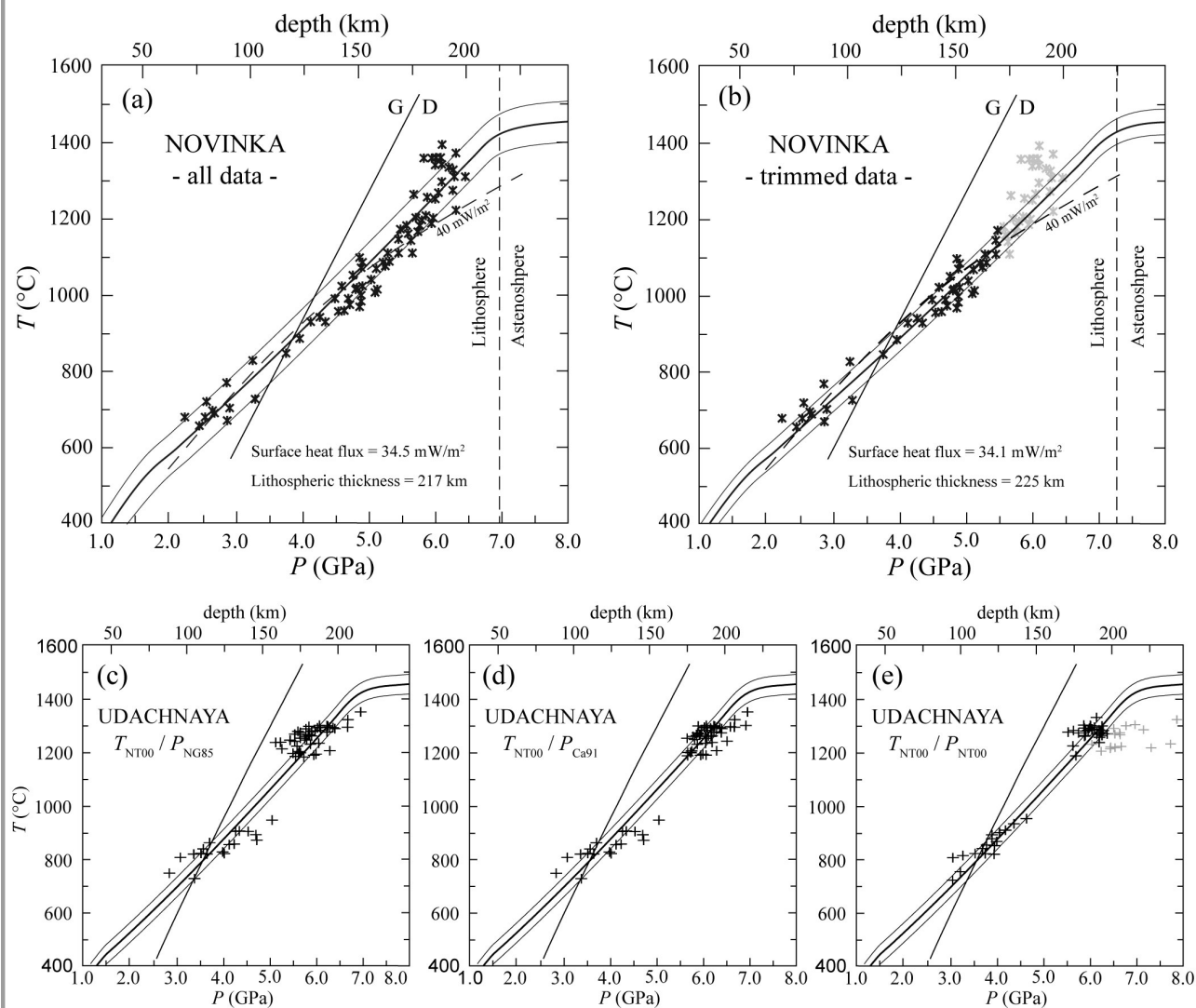
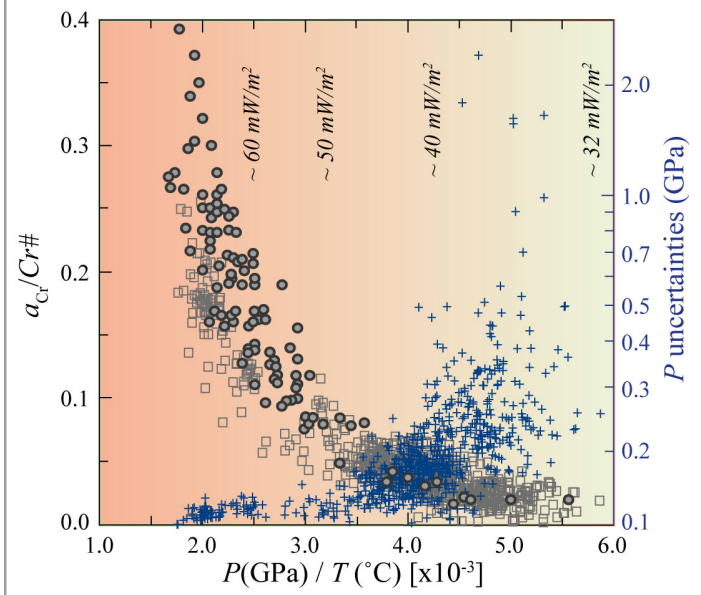


Figure 7



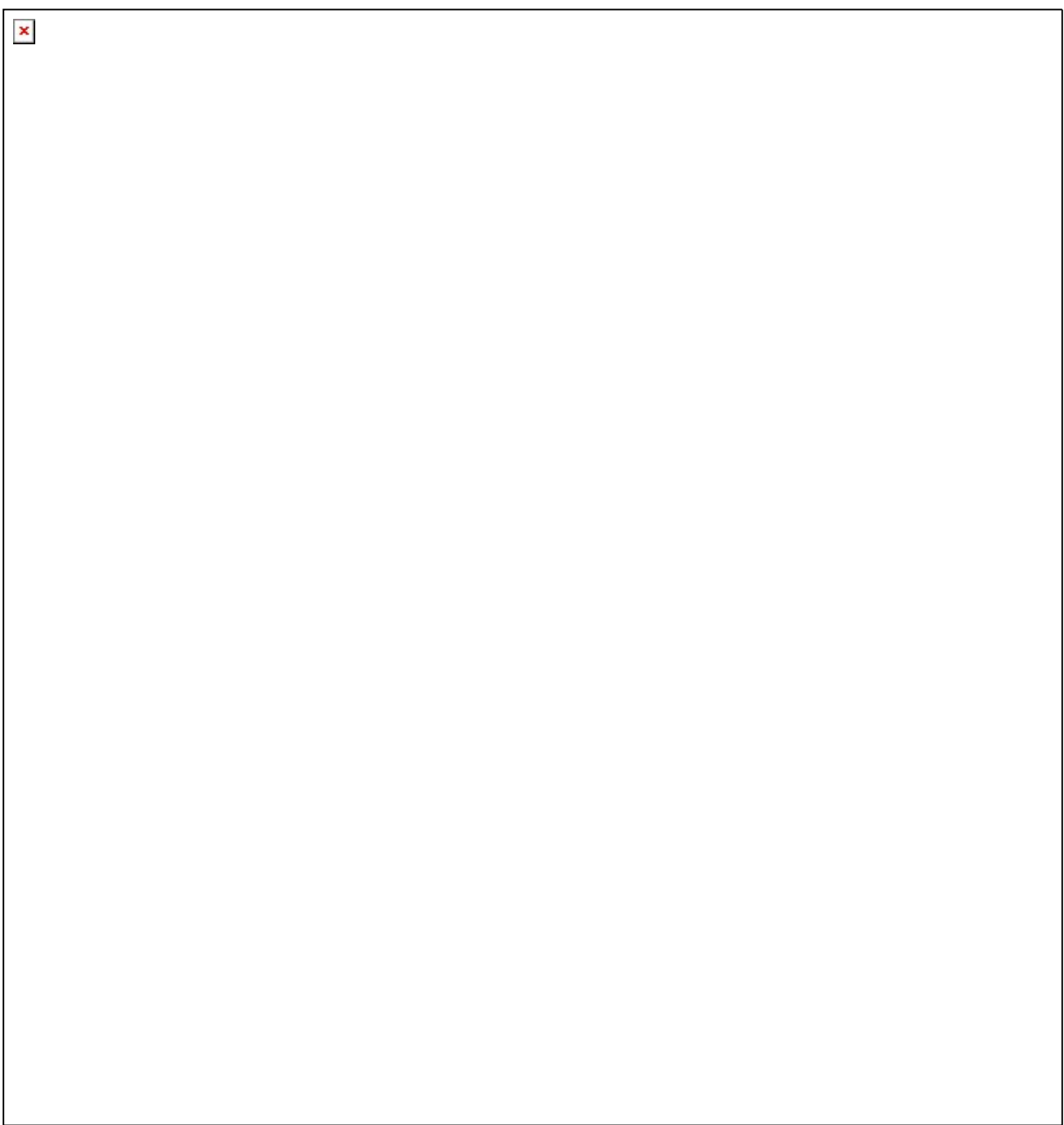


Table A1. Compositions (15 nA, 20 kV, 10 s peak + 10 s background) of clinopyroxenes used for the evaluation of propagation of analytical errors.

Sample	Nov-42	Nov-69	Nov-80	Nov-114	FRB1031	KGG-65	Uv61/91
SiO₂	54.82	54.32	55.08	54.65	55.69	54.57	54.88
TiO₂	0.27	0.24	0.21	0.30	0.25	0.28	0.05
Al₂O₃	2.21	2.06	2.46	1.77	2.46	2.65	0.61
Cr₂O₃	1.17	2.42	0.61	1.28	1.32	2.4	0.94
FeO_{tot}	3.83	3.14	4.39	4.01	3.26	2.26	2.45
MnO	0.12	0.11	0.09	0.11	0.11	0.06	0.10
MgO	16.30	15.95	20.20	18.27	19.23	16.15	19.20
CaO	18.58	18.57	14.58	17.07	16.74	19.5	20.92
Na₂O	2.12	2.34	1.85	1.74	1.89	2.32	0.65
K₂O	0.04	0.03	0.03	0.04	0.03	< 0.02	< 0.02
Sum	99.47	99.18	99.51	99.23	100.95	100.19	99.80
 Cr#	 0.27	 0.44	 0.14	 0.33	 0.27	 0.39	 0.51
<i>a</i>_{Cr}	0.0016	0.0103	0.0023	0.0037	0.0092	0.0188	0.0081
<i>T</i>_{NT00} (°C)	1088	1006	1369	1265	1270	912	1180
<i>P</i>_{NT00} (GPa)	6.32	4.84	6.44	6.61	5.22	3.69	6.01
<i>T</i>_{Ta98} (°C)	-	-	-	-	1265	972	1190
<i>P</i>_{Ca91} (GPa)	-	-	-	-	5.62	3.84	6.09

NT00 – Nimis and Taylor (2000); Ta98 – Taylor (1998); Ca91 – Nickel and Green (1985) with modifications by Carswell (1991). *T*_{Ta98} and *P*_{Ca91} for source xenoliths calculated using orthopyroxene and garnet compositions after Boyd (personal communication), Canil and O'Neill (1996) and Franz et al. (1996) and clinopyroxene compositions reported here.

Table A2. Electron microprobe operating conditions for the different analytical sessions. Accelerating voltage was fixed to 20 kV. The last row indicates the minimum $a_{Cr}/Cr\#$ values required to maintain the propagated pressure uncertainties within ± 0.25 GPa (1σ) (see section 2 of the Appendix).

Session	15-10/10	15-20/20	15-40/40	40-10/10	40-20/20	40-40/40
Beam current (nA)	15	15	15	40	40	40
Peak (sec)	10	20	40	10	20	40
Background (sec)	5 + 5	10 + 10	20+20	5 + 5	10 + 10	20 + 20
$a_{Cr}/Cr\#$	0.024	0.018	0.015	0.018	0.013	0.011

Table A3. Results of analytical sessions on selected clinopyroxenes using different operating condition (cf. Table A2).

Sample	AC	N	CaO		Al ₂ O ₃		Cr ₂ O ₃		Na ₂ O		Cr#		<i>a_{Cr}</i>		<i>P</i>	
			av	1σ	av	1σ	av	1σ	av	1σ	av	1σ	av	1σ	av	1σ
Nov-42	1510	15*	18.86	0.12	2.23	0.05	1.12	0.05	2.21	0.06	0.25	0.01	0.0001	0.0012	7.15	1.07
	1520	15*	18.84	0.08	2.24	0.02	1.14	0.04	2.19	0.03	0.25	0.01	0.0006	0.0005	7.37	1.04
	1540	15	18.87	0.06	2.25	0.02	1.12	0.04	2.17	0.02	0.25	0.01	0.0008	0.0005	7.18	0.70
	4010	15	18.81	0.05	2.23	0.03	1.14	0.04	2.18	0.04	0.25	0.01	0.0005	0.0008	7.30	1.01
	4020	15	18.94	0.03	2.25	0.02	1.12	0.03	2.18	0.02	0.25	0.00	0.0006	0.0004	7.42	0.72
	4040	15	18.85	0.05	2.24	0.02	1.14	0.01	2.18	0.02	0.25	0.00	0.0008	0.0002	7.06	0.34
Nov-69	1510	15	18.88	0.10	2.06	0.04	2.32	0.09	2.38	0.07	0.43	0.01	0.0078	0.0023	5.12	0.33
	1520	15	18.77	0.10	2.05	0.03	2.39	0.04	2.36	0.04	0.44	0.01	0.0090	0.0013	4.97	0.16
	1540	15	18.76	0.06	2.06	0.02	2.36	0.04	2.38	0.03	0.43	0.00	0.0084	0.0007	5.02	0.10
	4010	15	18.72	0.07	2.06	0.03	2.37	0.04	2.37	0.04	0.44	0.01	0.0087	0.0011	5.00	0.13
	4020	15	18.80	0.06	2.05	0.02	2.41	0.04	2.38	0.02	0.44	0.00	0.0088	0.0007	4.99	0.07
	4040	15	18.70	0.03	2.07	0.02	2.38	0.04	2.36	0.01	0.44	0.00	0.0092	0.0007	4.93	0.06
Nov-80	1510	15	14.56	0.16	2.56	0.05	0.56	0.05	1.80	0.05	0.13	0.01	0.0027	0.0005	6.07	0.23
	1520	15	14.49	0.05	2.56	0.04	0.57	0.04	1.81	0.02	0.13	0.01	0.0028	0.0003	6.06	0.13
	1540	15	14.47	0.04	2.58	0.02	0.58	0.03	1.82	0.02	0.13	0.01	0.0029	0.0002	6.03	0.08
	4010	15	14.48	0.05	2.57	0.03	0.57	0.03	1.82	0.04	0.13	0.01	0.0028	0.0004	6.08	0.17
	4020	15	14.56	0.04	2.57	0.02	0.58	0.02	1.81	0.02	0.13	0.00	0.0029	0.0003	6.02	0.10
	4040	15	14.55	0.03	2.54	0.02	0.59	0.02	1.83	0.01	0.13	0.00	0.0027	0.0002	6.17	0.08
Nov114	1510	15	17.23	0.13	1.84	0.05	1.16	0.09	1.76	0.04	0.30	0.02	0.0029	0.0012	6.93	0.60
	1520	15	17.06	0.08	1.84	0.03	1.20	0.05	1.77	0.03	0.30	0.01	0.0032	0.0006	6.73	0.24
	1540	15	17.10	0.05	1.84	0.02	1.19	0.03	1.78	0.03	0.30	0.01	0.0031	0.0005	6.76	0.23
	4010	15	17.14	0.08	1.83	0.02	1.22	0.04	1.78	0.03	0.31	0.01	0.0032	0.0009	6.80	0.35
	4020	15	17.21	0.06	1.85	0.02	1.22	0.04	1.79	0.01	0.31	0.01	0.0032	0.0004	6.72	0.13
	4040	15	17.19	0.04	1.82	0.01	1.25	0.02	1.79	0.01	0.32	0.00	0.0034	0.0004	6.71	0.12
KGG65	1510	15	19.48	0.12	2.65	0.04	2.21	0.07	2.31	0.05	0.36	0.01	0.0162	0.0016	3.75	0.08
	1520	15	19.50	0.08	2.65	0.05	2.21	0.07	2.28	0.04	0.36	0.01	0.0167	0.0011	3.72	0.05
	1540	15	19.52	0.05	2.65	0.02	2.19	0.05	2.29	0.03	0.36	0.01	0.0162	0.0008	3.74	0.05
	4010	15	19.51	0.05	2.63	0.02	2.17	0.05	2.31	0.03	0.36	0.01	0.0154	0.0009	3.78	0.05
	4020	15	19.54	0.05	2.63	0.02	2.17	0.04	2.30	0.02	0.36	0.01	0.0155	0.0008	3.78	0.04
	4040	15	19.58	0.04	2.62	0.01	2.16	0.02	2.30	0.02	0.36	0.00	0.0153	0.0004	3.79	0.02

Table A3. Continued

Sample	AC	N	CaO		Al ₂ O ₃		Cr ₂ O ₃		Na ₂ O		Cr#		a_{Cr}		P	
			av	1 σ	av	1 σ	av	1 σ	av	1 σ	av	1 σ	av	1 σ	av	1 σ
FRB1031	1510	15	16.75	0.11	2.49	0.06	1.25	0.07	1.88	0.03	0.25	0.01	0.0083	0.0010	5.27	0.13
	1520	15	16.64	0.07	2.43	0.03	1.22	0.04	1.88	0.03	0.25	0.01	0.0076	0.0007	5.38	0.10
	1540	15	16.67	0.06	2.44	0.01	1.24	0.04	1.87	0.03	0.26	0.01	0.0081	0.0006	5.32	0.07
	4010	15	16.75	0.06	2.48	0.03	1.20	0.06	1.90	0.02	0.24	0.01	0.0076	0.0007	5.34	0.07
	4020	15	16.77	0.07	2.47	0.02	1.20	0.02	1.89	0.02	0.25	0.00	0.0076	0.0003	5.34	0.04
	4040	15	16.80	0.08	2.48	0.01	1.21	0.02	1.89	0.02	0.25	0.00	0.0076	0.0003	5.33	0.04
Uv6191	1510	15	20.97	0.13	0.61	0.02	0.79	0.05	0.67	0.04	0.47	0.02	0.0049	0.0014	6.51	0.41
	1520	15	20.94	0.08	0.62	0.03	0.79	0.05	0.67	0.02	0.46	0.01	0.0051	0.0012	6.42	0.26
	1540	15	21.01	0.07	0.62	0.02	0.79	0.03	0.67	0.01	0.46	0.01	0.0050	0.0006	6.43	0.12
	4010	15	20.96	0.10	0.60	0.02	0.79	0.02	0.67	0.03	0.47	0.01	0.0049	0.0012	6.49	0.28
	4020	15	20.98	0.10	0.61	0.01	0.79	0.02	0.67	0.02	0.47	0.01	0.0050	0.0007	6.44	0.17
	4040	15	20.98	0.10	0.61	0.01	0.79	0.02	0.67	0.01	0.47	0.01	0.0049	0.0005	6.45	0.09

AC: analytical condition (cf. Table A2); N: number of analyses; av and 1 σ are average value and standard deviation, respectively (wt% for oxides; apfu for a_{Cr} ; GPa for P)

* A few analyses of sample Nov-42 resulted in negative values of a_{Cr} and were therefore excluded for the calculation of the mean and standard deviation of a_{Cr} and P .

Table A4. Model relationships between analytical error (relative st. dev., *err*) and element concentration (*c*) calculated by fitting the results of the analytical test to a function of the type $err = a / \sqrt{c}$ (after Potts et al. 1983). Listed parameters are fitted *a* values for each oxide (wt%) or element (a.p.f.u.) relevant to single-clinopyroxene geobarometry and for each combination of analytical conditions (nA-peak s/bkg s).

	15-10/10	15-20/20	15-40/40	40-10/10	40-20/20	40-40/40
Al ₂ O ₃	3.15	2.68	1.74	2.09	1.59	0.99
Al	0.64	0.54	0.35	0.42	0.32	0.20
Cr ₂ O ₃	6.42	4.78	3.39	3.89	2.61	2.17
Cr	1.08	0.80	0.57	0.65	0.44	0.36
Na ₂ O	3.85	2.48	1.90	2.95	1.66	1.33
Na	1.02	0.65	0.50	0.77	0.43	0.35